NANO LETTERS

2007
Vol. 7, No. 11
3499−3503

Electronic Transport Properties of Individual Chemically Reduced Graphene Oxide Sheets

Cristina Gómez-Navarro,[†] R. Thomas Weitz,[†] Alexander M. Bittner,[†] Matteo Scolari,[‡] Alf Mews,[‡] Marko Burghard,*[,†] and Klaus Kern[†,§]

Max-Planck-Institut fuer Festkoerperforschung, Heisenbergstrasse 1, 70569 Stuttgart, Germany, Department of Chemistry, University of Siegen, D-57068 Siegen, Germany, and Ecole Polytechnique Fédérale de Lausanne (EPFL), CH-1015 Lausanne, Switzerland

Received August 20, 2007; Revised Manuscript Received September 26, 2007

ABSTRACT

Individual graphene oxide sheets subjected to chemical reduction were electrically characterized as a function of temperature and external electric fields. The fully reduced monolayers exhibited conductivities ranging between 0.05 and 2 S/cm and field effect mobilities of 2–200 cm^2/Vs at room temperature. Temperature-dependent electrical measurements and Raman spectroscopic investigations suggest that charge transport occurs via variable range hopping between intact graphene islands with sizes on the order of several nanometers. Furthermore, the comparative study of multilayered sheets revealed that the conductivity of the undermost layer is reduced by a factor of more than 2 as a consequence of the interaction with the Si/SiO_2 substrate.

The peculiar electronic properties of graphene sheets have attracted strong interest both in the experimental and theoretical scientific community during the past few years.[1−3] Most prominently, carriers in an ideal graphene sheet behave as massless Dirac fermions.[4] In the meanwhile, these unique properties could be verified by a range of experiments,[4,5] and the first prototype devices such as field-effect transistors (FETs)[6] and ultra-sensitive sensors[7] have been successfully demonstrated. Micromechanical cleavage is currently the most effective and reliable method to produce high-quality graphene sheets.[8] However, the low yield of this approach (a few graphene monolayers per mm^2 of substrate area), combined with the lack of methods that enable positioning of the sheets, severely limits the implementation of highly integrated graphene-based circuits.

High-yield production methods for graphene sheets are also desirable for other applications like mechanically reinforced composites[9,10] or transparent, electrically conductive films.[11] A promising methodology is the chemical reduction of graphite oxide,[9,12,13] wherein the basal plane carbon atoms are decorated with epoxide and hydroxyl groups and the edge atoms bear carbonyl and carboxyl groups.[13−15] The presence of these functional groups reduces the interplane forces and imparts hydrophilic character, thereby promoting complete exfoliation of single graphene oxide (GO) layers in aqueous media. While no high-resolution microscopic data are available for GO, theoretical studies suggest that the oxygen-containing groups are clustered into rows and islands, resulting in graphitic regions intermixed with islands of oxygen-functionalized atoms.[16] Deoxygenation of GO has been accomplished by the strong chemical reducing agent hydrazine, whereupon a significant fraction of the contained oxygen is removed.[12,17] However, the electrical properties of reduced GO have remained largely unexplored, despite their relevance for evaluating the viability of this chemical route to graphene, as well as for the development of graphene-based conductive composites. In this report, we describe electronic transport studies of individual single- and multiple-layer GO sheets subjected to two different types of chemical reduction. The comparison with unmodified graphene demonstrates that such procedures enable only partial recovery of the electrical conductivity due to the oxidatively introduced point defects that remain within the 2D carbon framework.

Graphite oxide was prepared via the Hummers method,[18] starting from graphite flakes of 20 μm size (Sigma Aldrich). The resulting oxidized material was dispersed in water with the aid of soft ultrasonication and then deposited onto different substrates, including mica, Si/SiO_2, and highly oriented pyrolytic graphite (HOPG). While deposition onto mica and HOPG did not require any functionalization, the

[†] Max-Planck-Institut fuer Festkoerperforschung.
[‡] University of Siegen.
[§] Ecole Polytechnique Fédérale de Lausanne (EPFL).

10.1021/nl072090c CCC: $37.00
Published on Web 10/18/2007

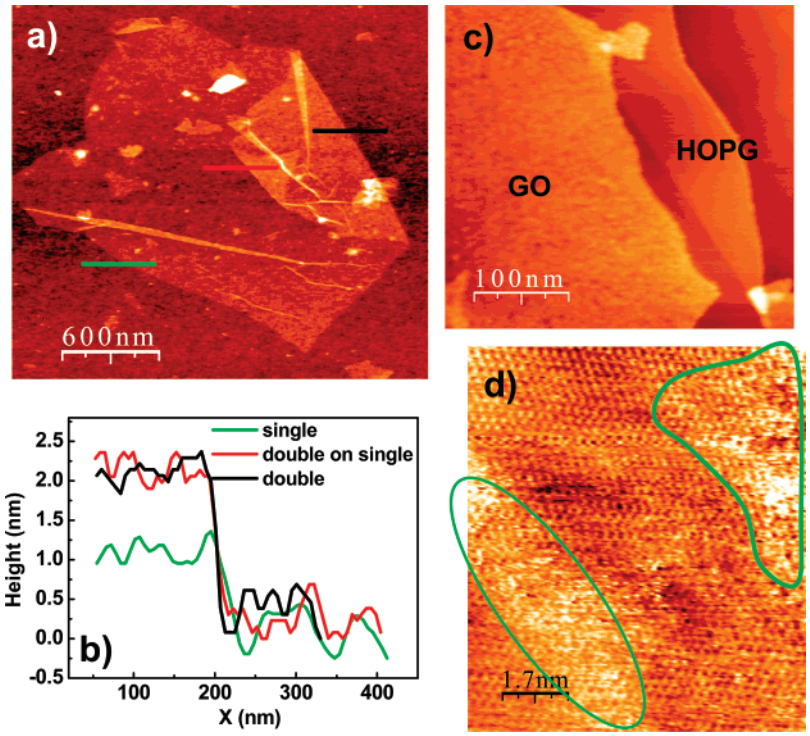

Figure 1. (a) AFM image of a GO monolayer deposited on a SiO_2 substrate, showing a back-folded edge. (b) AFM section profiles along the three different lines in panel (a), revealing a mono-, bi-, and trilayer structure. (c) AFM image acquired from a GO monolayer on a HOPG substrate. (d) STM image of a GO monolayer on a HOPG substrate, taken under ambient conditions. Oxidized regions are marked by green contours.

surface of the Si/SiO_2 substrates was modified by 3-aminopropyltriethoxysilane (APTES) prior to deposition. Figure 1a displays an atomic force microscopy (AFM) image of a GO sheet whose upper right edge is double-folded onto itself, as can be concluded from the cross-sectional profiles depicted in Figure 1b. Analysis of a larger number of AFM images[19] revealed GO sheets with lateral dimensions of 100−5000 nm and heights in the range of 1.1−15 nm. Approximately 80% of the sheets displayed a height of 1.1 ± 0.2 nm, and multiples of this value were found for the remaining objects. This height, being somewhat larger than the value of 0.8 nm predicted by theory,[13] has been observed also by other AFM studies[12,13] and assigned to individual graphitic sheets bearing oxygen-containing groups on both faces. AFM images of the GO monolayers on atomically flat surfaces like mica or HOPG, as shown in Figure 1c, disclose a pronounced roughness which considerably exceeds that of the substrate. This feature can be attributed to sp^3 centers and point defects in the carbon lattice that cause wrinkling of the sheets on the nanometer scale.[13,14] In order to gain further structural information, the GO sheets were examined by scanning tunneling microscopy (STM) under ambient conditions. As exemplified by the STM image of a GO monolayer shown in Figure 1d, the hexagonal lattice of the sheets turns out to be partially preserved. The STM images of the GO sheets are distinguishable from pristine graphene by the appearance of bright spots/regions lacking ordered lattice features. They most likely arise from the presence of oxygenated functional groups, which are predicted by theory to arrange into islands and rows.[16] The functionalization degree was estimated from a range of STM images to be approximately 50%, in fair agreement with the oxygen content of ∼70% determined by spectroscopic analysis of GO.[12]

For the aim of further characterization, confocal Raman spectroscopy was performed on single GO monolayers before and after chemical reduction. To this end, two different reduction methods were employed. The first method involved immersion of the solid-supported sheets into a 1 vol% hydrazine solution in dimethylformamide (DMF) at 80 °C for 24 h. Alternatively, the samples were exposed to hydrogen plasma (30 W at a pressure of 0.8 mbar) for 5−10 s at room temperature. The Raman spectrum of the as-prepared GO sheets (Figure 2) displays two prominent peaks at 1340 and 1600 cm^{-1}, which correspond to the well-documented D and G band, respectively.[20] The appearance of the D band in sheets with lateral dimensions much larger than the laser spot (∼400 nm) signifies disorder in the carbon lattice. The intensity ratio of the D and G band is a measure of the disorder, as expressed by the sp^2/sp^3 carbon ratio.[21] By using the empirical Tuinstra−Koenig relation,[22] which relates the D/G intensity ratio to the crystallite size of graphitic samples, it can be concluded that the GO sheets are comprised of ordered graphitic regions with a size of ∼6 nm surrounded by areas of oxidized carbon atoms or point defects. This value is in reasonable agreement with the size of intact areas as observed in our STM images. Intriguingly, after chemical reduction, the sheets did not show any noticeable decrease in the D/G ratio. This observation suggests that while most of the oxygenated groups are removed, the vacant lattice sites produced via carbon atom removal in the form of CO or CO_2 during graphite oxidation

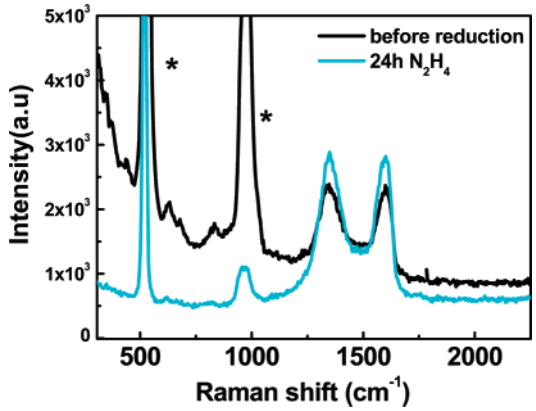

Figure 2. Raman spectrum of two different individual GO monolayers before and after reduction by hydrazine, recorded with $\lambda_{exc} = 514$ nm. The lateral sheet dimension was 2 μm, in order to avoid edge effects. Peaks marked by an asterisk originated from the Si substrate.

remain unchanged by the reduction process and predominantly define the intact graphene regions.

Toward their electrical characterization, the GO sheets were deposited on degenerately doped silicon substrates with a thermally grown SiO_2 layer (200 nm thickness), chemically reduced, and then contacted by e-beam lithographically defined Au/Pd (60/40) electrodes (300−1000 nm separation). Before reduction, the GO monolayers behaved close-to-insulating, with differential conductivity values of $1-5 \times 10^{-3}$ S/cm at a bias voltage of 10 V (calculated assuming a layer thickness of 1 nm). Chemical reduction resulted in a pronounced increase of conductivity, as demonstrated by Figure 3. In the case of both reduction methods, the time evolution of conductivity displayed a plateau, followed by a decrease upon further exposure. This plateau was respectively reached after 24 h and 5 s for hydrazine and hydrogen plasma treatment. In the following, when speaking of "reduced GO", we refer to sheets subjected to these respective reduction times in order to ensure the maximum attainable reduction degree. The conductivity of the reduced GO monolayers was found to be approximately 3 orders of magnitude higher compared to the starting GO. Room-temperature measurements of more than 50 reduced GO monolayers yielded conductivity values between 0.05 and 2 S/cm. This range is about 3 orders of magnitude below the values reported for pristine graphene.[1,2] It is worthy to note that even on the same substrate, the conductivity of different monolayers varied by up to 1 order of magnitude.

The reduced GO samples showed a significant conductivity decrease by more than 3 orders of magnitude upon cooling from 298 to 4 K, in contrast to unmodified graphene whose conductivity was reduced by less than 1 order of magnitude.[1,23] Best linear fits of the temperature-dependent data were obtained by plotting $\ln(I/A)$ versus $T^{-1/3}$ (Figure 4a), pointing toward variable range hopping (VRH) as a plausible charge-transport mechanism in the reduced GO sheets. VRH involves consecutive inelastic tunneling processes between two localized states and has been frequently observed in disordered systems, including amorphous carbon.[24] It obeys the following general temperature dependence: $I = I_0 e^{-(T_0/T)^{1/n}}$, where $(n - 1)$ is the dimensionality of the sample.[25] The two-dimensional (2D) character reflected by the observed $\propto T^{1/3}$ dependence is consistent with the 2D structure of the sheets. In view of the above-described Raman results, hopping presumably occurs between the intact graphene regions which are separated by clusters of point defects.

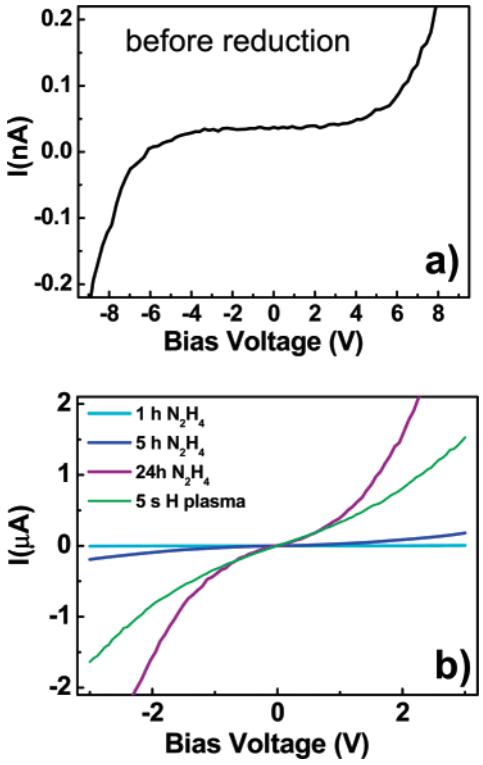

Figure 3. Room-temperature $I-V$ curves acquired under ambient conditions of (a) an as-prepared GO monolayer and (b) individual GO monolayers chemically reduced by hydrazine (for 1, 5, and 24 h) and hydrogen plasma (5 s) treatment. All samples were contacted by electrodes with a separation of 300 nm.

Despite their different temperature dependence of electrical conductivity, the reduced GO monolayers showed ambipolar behavior in the gate dependence of resistance (Figure 4b) similar to that of pristine graphene.[1] The presented data were collected within a cryostat under a low pressure of helium, which explains the fact that the resistance maxima occur close to zero gate voltage. Prolonged exposure of the samples to the ambient (>24 h) resulted in a pronounced shift of the maxima toward positive gate voltages, which could be reversed by placing them back in vacuum. Comparable shifts observed for graphene and single-walled carbon nanotubes have been attributed to doping by oxygen and/or water absorption.[1,26] Room-temperature field-effect mobilities of 2−200 cm^2/Vs for holes and 0.5−30 cm^2/Vs for electrons were extracted from the gate dependence of resistance[1] of the reduced GO samples. As a consequence of the defective nature of the reduced layers, these values are approximately 2 orders of magnitude lower than those of graphene, for which mobilities between 3000 and 10000 cm^2/Vs have been reported.[1,6] The principal similarity between the gate dependence of the reduced GO and graphene is a direct indication of the presence of intact graphitic domains in the former

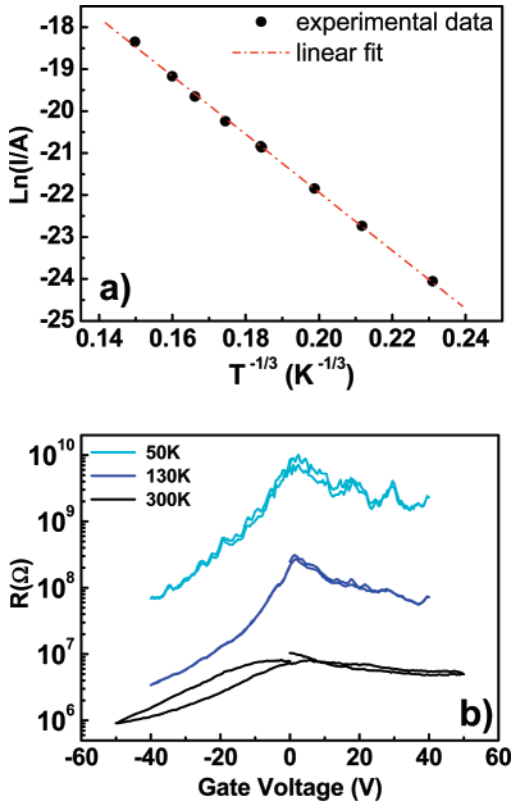

Figure 4. (a) Semilogarithmic plot of current (I) versus $T^{-1/3}$ of a fully reduced GO monolayer ($V_{bias} = 0.2$ V). (b) Low-bias resistance of a fully reduced GO monolayer measured as a function of back gate voltage at three different temperatures ($V_{bias} = \pm 100$ mV).

material. For further increased defect density, hopping between neighboring atomic sites would be expected to occur over the entire sample, associated with a rather weak gate dependence of resistance typical of such systems.[27]

Finally, we have extended the electrical measurements to multilayered GO sheets. Due to the sizable conductivity variation between different samples, we first selected partially folded sheets that allow simultaneous contacting of a mono- and bilayer configuration, like the one shown in Figure 5a. In these experiments, the low-bias conductivity measured for the bilayer reproducibly exceeded that of the first layer by more than a factor of 2. Assuming the validity of the simple electrical circuits inserted in the figure (i.e., charge is transported through parallel resistors with negligible vertical conduction) and that the resistance of the first layer remains identical to the monolayer case, we concluded that the second layer is more conducting than the first one by factors between 2 and 5. In order to expand the study to multilayered sheets, we then performed a statistical analysis over a range of samples. As apparent from Figure 6, no further increase in (volume) conductivity could be detected for sheets containing between 3 and 7 layers, which supports the above assumption and, furthermore, provides evidence that the conduction in the first layer is limited by the interaction with the substrate. This interaction may include the influence of amino groups contained in the APTES layer used for modifying the SiO_2 surface. Such substrate interactions may account for the differences we observed from sheet

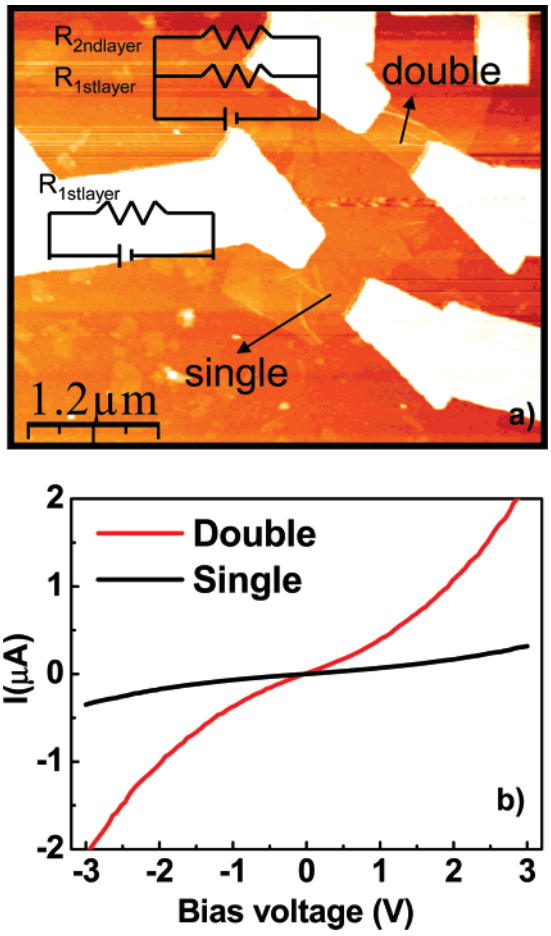

Figure 5. (a) AFM image of a chemically reduced GO layer with electrical contact pairs attached to a mono- and bilayer region. The inset shows the simple electronic circuit used for data evaluation. (b) $I-V$ curves obtained under ambient conditions from the mono- and bilayer configurations of panel (a) at zero gate voltage.

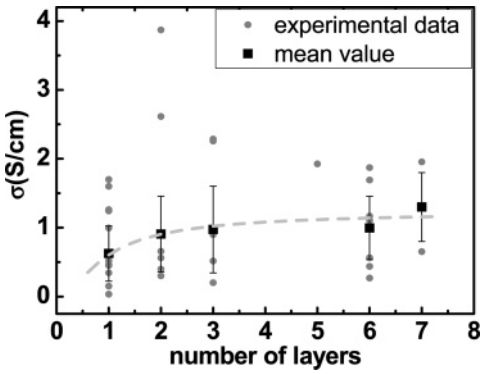

Figure 6. (a) Plot of the mean volume conductivity (measured under ambient conditions) as a function of the number of layers within fully reduced GO sheets. The gray dashed line has been drawn as a guide for the eye.

to sheet and, likewise, for those reported for graphene prepared through mechanical exfoliation.[1] In this context, it is interesting to note that thermal annealing of the reduced GO sheets in vacuum at 500 °C decreases the resistance of bilayers but does not influence the monolayers. This difference suggests that the substrate interaction also restricts healing processes requiring atomic diffusion, which may be

responsible for the observed resistance decrease in the bilayer case. Additional interference may arise from defects in the SiO_2 layer that survive the annealing procedure.

In summary, we have presented the first electronic transport studies of chemically reduced graphene oxide sheets, which potentially provide access to large-scale production of graphene monolayers. In the fully reduced sheets, the room-temperature conductivity and carrier mobility were found to lag behind those of graphene by 3 and 2 orders of magnitude, respectively, predominantly as a consequence of lattice vacancies that cannot be healed during the reduction process. The structure of the sheets is best described by intact, nanometer-sized graphitic domains separated by defect clusters, which results in hopping conduction as the dominant charge-transport mechanism. Future high-resolution microscopic investigations could reveal further details about the defect nature and identify the location of oxygenated functionalities which presumably remain in a low concentration. Such knowledge would be of relevance for attempts to tune the electronic structure of graphene via chemical edge functionalization.[28,29]

Acknowledgment. C. Gómez-Navarro appreciates support by the Alexander-von-Humboldt Foundation.

References

(1) Novoselov, K. S.; Geim, A. K.; Morozov, S. V.; Jiang, D.; Zhang, Y.; Dubonos, S. V.; Grigorieva, I. V.; Firsov, A. A. *Science* **2004**, *306*, 666.
(2) Berger, C.; Song, Z. M.; Li, X. B.; Wu, X. S.; Brown, N.; Naud, C.; Mayo, D.; Li, T. B.; Hass, J.; Marchenkov, A. N.; Conrad, E. H.; First, P. N.; de Heer, W. A. *Science* **2006**, *312*, 1191.
(3) Geim, A. K.; Novoselov, K. S. *Nat. Mater.* **2007**, *6*, 183.
(4) Novoselov, K. S.; Geim, A. K.; Morozov, S. V.; Jiang, D.; Katsnelson, M. I.; Grigorieva, I. V.; Dubonos, S. V.; Firsov, A. A. *Nature* **2005**, *438*, 197.
(5) Zhang, Y. B.; Tan, Y. W.; Stormer, H. L.; Kim, P. *Nature* **2005**, *438*, 201.
(6) Lemme, M. C.; Echtermeyer, T. J.; Baus, M.; Kurz, H. *IEEE Electron Device Lett.* **2007**, *28*, 282.
(7) Schedin, F.; Geim, A. K.; Morozov, S. V.; Hill, E. W.; Blake, P.; Katsnelson, M. I.; Novoselov, K. S. *Nat. Mater.* **2007**, *6*, 652.
(8) Novoselov, K. S.; Jiang, D.; Schedin, F.; Booth, T. J.; Khotkevich, V. V.; Morozov, S. V.; Geim, A. K. *Proc. Natl. Acad. Sci. U.S.A.* **2005**, *102*, 10451.
(9) Stankovich, S.; Dikin, D. A.; Dommett, G. H. B.; Kohlhaas, K. M.; Zimney, E. J.; Stach, E. A.; Piner, R. D.; Nguyen, S. T.; Ruoff, R. S. *Nature* **2006**, *442*, 282.
(10) Dikin, D. A.; Stankovich, S.; Zimney, E. J.; Piner, R. D.; Dommett, G. H. B.; Evmenenko, G.; Nguyen, S. T.; Ruoff, R. S. *Nature* **2007**, *448*, 457.
(11) Watcharotone, S.; Dikin, D. A.; Stankovich, S.; Piner, R.; Jung, I.; Dommett, G. H. B.; Evmenenko, G.; Wu, S.-E.; Chen, S.-F.; Liu, C.-P.; Nguyen, S. T.; Ruoff, R. S. *Nano Lett.* **2007**, *7*, 1888.
(12) Stankovich, S.; Piner, R. D.; Chen, X. Q.; Wu, N. Q.; Nguyen, S. T.; Ruoff, R. S. *J. Mater. Chem.* **2006**, *16*, 155.
(13) Schniepp, H. C.; Li, J. L.; McAllister, M. J.; Sai, H.; Herrera-Alonso, M.; Adamson, D. H.; Prud'homme, R. K.; Car, R.; Saville, D. A.; Aksay, I. A. *J. Phys. Chem. B* **2006**, *110*, 8535.
(14) Lerf, A.; He, H. Y.; Forster, M.; Klinowski, J. *J. Phys. Chem. B* **1998**, *102*, 4477.
(15) He, H. Y.; Klinowski, J.; Forster, M.; Lerf, A. *Chem. Phys. Lett.* **1998**, *287*, 53.
(16) Li, J. L.; Kudin, K. N.; McAllister, M. J.; Prud'homme, R. K.; Aksay, I. A.; Car, R. *Phys. Rev. Lett.* **2006**, *96*, 176101.
(17) Stankovich, S.; Dikin, D. A.; Piner, R. D.; Kohlhaas, K. A.; Kleinhammes, A.; Jia, Y.; Wu, Y.; Nguyen, S. T.; Ruoff, R. S. *Carbon* **2007**, *45*, 1558.
(18) Hummers, W. S.; Offeman, R. E. *J. Am. Chem. Soc.* **1958**, *80*, 1339.
(19) The analysis of AFM images was made using the software WSxM described in: Horcas, I.; Fernandez, R.; Gomez-Rodriguez, J. M.; Colchero, J.; Gomez-Herrero, J.; Baro, A. M. *Rev. Sci. Instrum.* **2007**, *78*, 013705.
(20) Pimenta, M. A.; Dresselhaus, G.; Dresselhaus, M. S.; Cancado, L. G.; Jorio, A.; Saito, R. *Phys. Chem. Chem. Phys.* **2007**, *9*, 1276.
(21) Ferrari, A. C.; Robertson, J. *Phys. Rev. B* **2000**, *61*, 14095.
(22) Tuinstra, F.; Koenig, J. L. *J. Chem. Phys.* **1970**, *53*, 1126.
(23) Tan, Y.-W.; Zhang, Y.; Stormer, H. L.; Kim, P. *Eur. Phys. J.* **2007**, *148*, 15.
(24) Robertson, J. *Adv. Phys.* **1986**, *35*, 317.
(25) Mott, N. F.; A Davis, E. *Electronic Processes in Non-Crystalline Materials*; Oxford University Press: Oxford, England, 1971.
(26) Martel, R.; Derycke, V.; Lavoie, C.; Appenzeller, J.; Chan, K. K.; Tersoff, J.; Avouris, P. *Phys. Rev. Lett.* **2001**, *87*, 256805.
(27) Kim, G. T.; Muster, J.; Krstic, V.; Park, J. G.; Park, Y. W.; Roth, S.; Burghard, M. *Appl. Phys. Lett.* **2000**, *76*, 1875.
(28) Son, Y. W.; Cohen, M. L.; Louie, S. G. *Phys. Rev. Lett.* **2007**, *98*, 089901.
(29) Wang, Z. F.; Li, Q. X.; Zheng, H. X.; Ren, H.; Su, H. B.; Shi, Q. W.; Chen, J. *Phys. Rev. B* **2007**, *75*, 113406.

NL072090C